Non-equilibrium distribution of kinesin-streptavidin complexes revealed by Mass Photometry

Jing Xu,*[a] Nathaniel J. S. Brown,[b] Yeonee Seol[c] and Keir C. Neuman[c]

[a] Department of Physics, University of California, Merced, CA 95343, USA

[b] Department of Quantitative and Systems Biology, University of California, Merced, CA 95343, USA

[c] Laboratory of Single Molecule Biophysics, National Heart, Lung and Blood Institute, NIH, Bethesda, MD 20892, USA

* Correspondence: jxu8@ucmerced.edu

Abstract

Kinesin-streptavidin complexes are widely used in microtubule-based active-matter studies. The stoichiometry of the complexes, formed under non-equilibrium conditions, is empirically tuned but the distribution has not been experimentally determined. Here we directly measure the distribution of kinesin-streptavidin complexes via mass photometry. We identify conditions that maximize the desired complex stoichiometry.

Kinesin-streptavidin complexes are widely used to drive filament-filament sliding in microtubule-based active matter studies[1-7]. The complexes are typically formed via incubating biotinylated kinesin dimers with streptavidin tetramers. Each kinesin dimer contains up to two copies of engineered biotin tags at its C-terminus[8, 9], and each streptavidin tetramer can bind up to four biotins. The molar ratio of kinesin dimers and streptavidin tetramers is empirically tuned to optimize key characteristics of the resulting active matter[1, 3]. The resulting complexes are generally assumed to contain two kinesin dimers and one streptavidin tetramer, corresponding to a 2:1 complex stoichiometry. Although this complex stoichiometry is often assumed in theoretical modelling of microtubule-based active matter, it has not been experimentally verified. Importantly, the tetravalence of streptavidin and bivalence of kinesin can produce heterogenous, rather than homogenous, complex populations, for example allowing up to four kinesin dimers on a single streptavidin tetramer, or up to two streptavidin tetramers on each kinesin dimer. Indeed, an early study found evidence of up to 8 kinesin dimers per complex[7]. The relative abundance of the complex, however, was not determined.

In principle, heterogeneous distributions of complexes could be estimated based on the molar ratio of proteins used in the incubation ("incubation ratio"). This would require assumptions concerning the relative probability of kinesin dimers binding via one or both biotins. However, these estimates require that the complex formation has reached thermodynamic equilibrium, which is not the case for the kinesin-streptavidin complexes in active-matter studies. Biotin-streptavidin binding is one of the strongest non-covalent interactions in nature, with exceptionally slow dissociation kinetics (~10^{-6} s^{-1} at room temperature[10, 11]) and thus an exceptionally long time to reach thermodynamic equilibrium (~50 days at room temperature based on the dissociation kinetics). This extended equilibrium time is not practical, given that it is substantially longer than the duration for which kinesin motor proteins remain active in aqueous solution[12]. As a result, kinesin-streptavidin complexes are typically formed under non-equilibrium conditions (~30 min incubation on ice in standard protocols), resulting in non-equilibrium distributions that are not readily determined based on the incubation ratio.

Quantitative characterization of kinesin-streptavidin complexes is experimentally challenging. For example, the relatively high concentrations of proteins required for analytical gel filtration or ultracentrifugation can induce non-specific aggregates that are otherwise not present at the sub-µM concentrations employed in active-matter work. Although dynamic light scattering can detect particle sizes at dilute concentrations, the resulting size distribution is weighted by scattering intensity and estimates of relative abundance in a heterogeneous population are highly model-dependent[13, 14]. Finally, fluorescence-based methods, such as stepwise photobleaching, are complicated by incomplete fluorescence-labelling of proteins[15].

Here we employ mass photometry measurements to quantitatively determine the non-equilibrium distribution of kinesin-streptavidin complexes (Fig. 1). Mass photometry is a recently-developed, label-free, technique that utilizes interferometric light scattering[16-19] to determine the mass of proteins and protein complexes in solution[20]. Briefly, scattered light from protein complexes at the glass-buffer interface interferes with light reflected from the same interface (Fig. 1a). The resulting interference intensity scales linearly with the molecular

mass of the protein complex. Heterogeneity in interference intensities reveal multiple species of protein complexes in solution (Fig. 1b, bottom panel). Moreover, the working concentration of mass photometry (0.1–100 nM[21, 22]) is dilute but well above the dissociation constant of biotin-streptavidin binding (~10^{-14} M[23, 24]), preserving the complex integrity while avoiding protein aggregation. The broad detection range of mass photometry (~50–5000 kDa)[21, 22] is also well-suited for characterizing heterogeneous populations of kinesin-streptavidin complexes with different stoichiometries.

We prepared kinesin-streptavidin complexes following standard protocols[6] over a range of incubation ratios common in active-matter studies[1-7] (Materials and Methods, ESI†). Unless otherwise noted, the concentration of streptavidin tetramers was kept constant at 0.6 μM, and the concentration of kinesin dimers was varied. Solutions containing only kinesin dimers or streptavidin tetramers were used as controls. Mass photometry experiments were carried out using a OneMP instrument (Refeyn, UK) (Materials and Methods, ESI†). Intensity of individual complexes in mass photometry images (for example, Fig. 1b) were converted to molecular mass via calibrations with known masses[20, 22]. Results were pooled to determine the distribution of molecular masses in each protein solution (Fig. 2). Major species were identified by fitting the associated mass distributions to a bi-Gaussian mixture model (solid red lines, Fig. 2), the molecular mass and abundance of each species was calculated based on the best-fit parameters (Materials and Methods, ESI†).

We detected single mass species in control solutions that contained only a single protein (top two panels, Fig. 2a). The molecular masses of each species are in good agreement with the theoretical masses of the streptavidin tetramer or the kinesin dimer (i-ii, Fig. 3), as well as a prior mass photometry measurement of the streptavidin tetramer (57.2 ± 1.5 kDa in the current study *vs*. 55.7 ± 1.1 kDa previously[20]). These results validate the accuracy of mass photometry and demonstrate no significant protein aggregates in either control solutions.

In contrast, we detected multiple mass species in solutions containing both kinesin and streptavidin (bottom six panels, Fig. 2a and 2b). In addition to the two isolated proteins in control solutions, mass photometry revealed three larger species (iii-v, Figs. 2a and 2b). The molecular masses of these larger species are highly correlated with theoretical molecular masses for complexes containing up to three kinesin dimers and one streptavidin tetramer (iii-v, Fig. 3). Note that the correspondence between molecular mass and complex stoichiometry is not necessarily unique, given that the molecular mass of our kinesin dimer is approximately twice that of a streptavidin tetramer. For example, the measured mass of species iv could, in principle, be consistent with a complex containing one kinesin dimer and three streptavidin tetramers (~271 kDa). However, this possibility is unlikely given that the complex was observed in solutions with excess kinesin (Fig. 2b). In addition to complex species iii-v, we also detected substantially larger species that we refer to as "higher-order complexes" (Fig. S1, ESI†). These higher-order complexes likely comprise a mixture of different species; the mass at ~950 kDa (Fig. S1, ESI†) is consistent with an early report that complexes could contain up to 8 kinesin dimers[7].

Interestingly, for most incubation ratios tested, we detected mainly the isolated proteins rather than kinesin-streptavidin complexes (Fig. 2a). This observation is not due to detection limitations: substantial populations of kinesin-streptavidin complexes were detected at an incubation ratio of 1.6 kinesins per streptavidin (K:S 1.6:1, Fig. 2a and 2b). Instead, this result likely reflects the fact that the complexes were prepared under non-equilibrium conditions[10]. Additionally, the biotin- streptavidin association kinetics may be slower for protein-associated biotins than that established for free biotin streptavidin association kinetics may be slower for protein- associated biotins than that established for free biotin molecules, potentially due to increased steric effects and/or reduced diffusion of biotin attached to kinesin dimers.

Looking at more detail in the region of complex species (Fig. 2b), we observed more than one complex species in most kinesin-streptavidin solutions (bottom five panels, Fig. 2b). The relative abundance of each complex species varied as we varied the incubation ratio of kinesin to streptavidin (Fig. 2b). These observations demonstrate that the non-equilibrium populations of kinesin-streptavidin complexes are heterogenous, and that the heterogeneity depends highly on the incubation ratio. It has long been established that that the kinesin: streptavidin incubation ratio dictates the key characteristics of active matter[1, 3]. Our data here suggests that the characteristics of active matter depend sensitively on the relative abundance of each complex species.

We next determined the relative abundance of different species of kinesin-streptavidin complexes (Fig. 4). Here we focused on individual complex species with well-defined stoichiometries (top three panels, Fig. 4) and cumulative contributions from higher-order complexes (bottom panel, Fig. 4). Isolated proteins were not included in this calculation. As the incubation ratio increased, the abundance of complexes containing one kinesin decreased (top panel, Fig. 4), and the relative abundances of complexes with two or more kinesins increased (bottom three panels, Fig. 4). Of note, the relative abundance varied when we varied the concentrations of kinesin and streptavidin but kept their incubation ratio constant (Fig. S2, ESI†). This observation again highlights the non-equilibrium nature of the kinesin-streptavidin complex formation and demonstrates the importance of direct measurements of complex distribution.

We found that an incubation ratio of ~1.6-1.7 kinesin dimers per streptavidin tetramer maximizes the relative abundance of the 2:1 complex stoichiometry and minimizes the probability of larger complexes (grey region, Fig. 4). Below this incubation ratio, the most abundant complex contains one kinesin dimer and one streptavidin (top panel, Fig. 4), which is functionally equivalent to a single kinesin dimer and cannot drive pair-wise sliding of filaments in active matter. Above this incubation ratio, the relative abundance of larger complexes increases (bottom two panel, Fig. 4), which could have varied influences on the dynamics of active matter. Nonetheless, at this optimal incubation ratio, our measurements of complex distribution reveal a substantial fraction of complexes with three or more kinesin dimers (bottom two panels, Fig. 4).

Conclusions

Here we employed mass photometry to determine the non-equilibrium distribution of kinesin-streptavidin complexes widely employed in microtubule-based active matter studies (Fig. 1). Our mass photometry measurements recovered the expected molecular masses for the isolated proteins and identified three main kinesin-streptavidin complexes (Figs. 2 and 3). The molecular masses of these three main species correspond to complexes containing up to three kinesin dimers and one streptavidin tetramer (Figs. 2 and 3). We also uncovered evidence of higher-order complexes reported previously[7] (Fig. S1, ESI†). We show that the complex population is heterogeneous, and this heterogeneity depended sensitively on the molar ratio and concentration of kinesin and streptavidin in the incubation (Figs. 2, 4, and S2, ESI†).

Our study provides a quantitative guide for estimating the stoichiometry and relative abundance of kinesin-streptavidin complexes prepared using standard active-matter protocols[6] (Figs. 2 and 4). To our knowledge, this is the first such guide. We identified an incubation ratio of ~1.6-1.7 kinesin per streptavidin that maximizes the desired 2:1 complex stoichiometry (Fig. 4). Our findings provide mechanistic insight for the prior finding that a similar incubation ratio of 1.7 kinesin dimers per streptavidin tetramer optimizes the key characteristics of microtubule-based active matter[3]. Moreover, our data provide for the first time a measure of the abundance of the larger complex species (for example, those with a 3:1 stoichiometry, Fig. 4) that could influence the dynamics of the system and could be included in models and analysis of active matter experiments. Finally, we anticipate that the mass photometry technique used in the current study may be broadly applicable for quantitative characterizations of other dynamic cross-linkers[25-28] in microtubule-based active matter.

Author Contributions

J. X. conceived and designed the study; J. X. and N. J. S. B. performed the experiments and analyzed the data; Y. S. generated the recombinant motor protein; J. X. wrote the manuscript. K. C. N. and Y. S. edited it. All the authors reviewed the paper.

Conflicts of interest

There are no conflicts to declare.

Acknowledgements

This work was supported by the National Institutes of Health (R15 GM120682 to J. X.) and the Intramural Research Program of the National Heart, Lung, and Blood Institute, National Institute of Health (ZIAHL001056 to K. C. N.).

We thank Di Wu, Grzegorz Piszczek, Duck-Yeon Lee, Yasuharu Takagi, and Adam Fineberg for support and comments. We thank the Biophysical Core Facility and the Biochemistry Core Facility for the use of the OneMP instrument and for providing mass spectroscopy measurements. We thank Zvonimir Dogic, Shibani Dalal, the Brandeis Biomaterials Facility, and the National Science Foundation grant no. DMR 2011846 for providing the K401-BIO-6H plasmid. We thank Esme P. Neuman for illustrations of kinesin dimer.

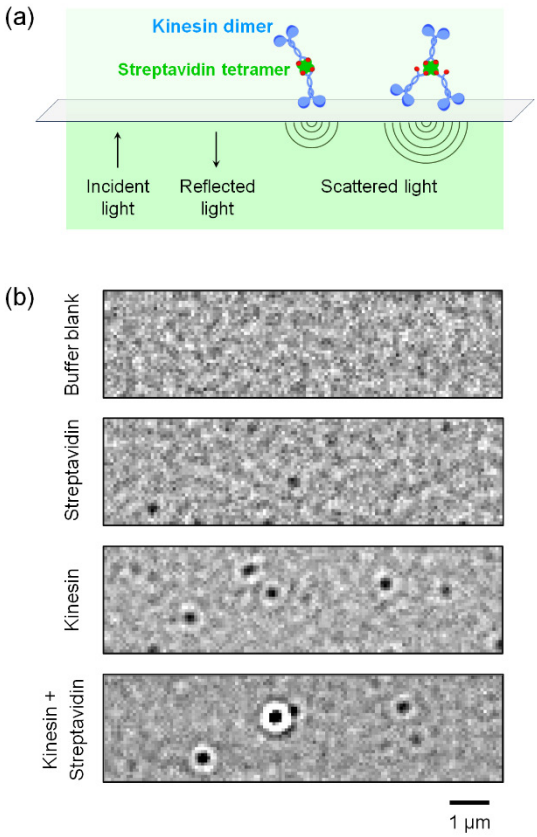

Figure 1 (a) Illustration of mass photometry experiments, in which scattered light from protein complexes on the glass surface interferes with reflected light from the same surface. Illustration is not to scale. (b) Representative mass photometry images of protein-free buffer (top) and protein solutions (bottom three panels). Scale bar, 1 µm. Interference intensity of each spot scales linearly with molecular mass; heterogeneity in spot intensities reveal multiple species of protein complexes in solution (bottom).

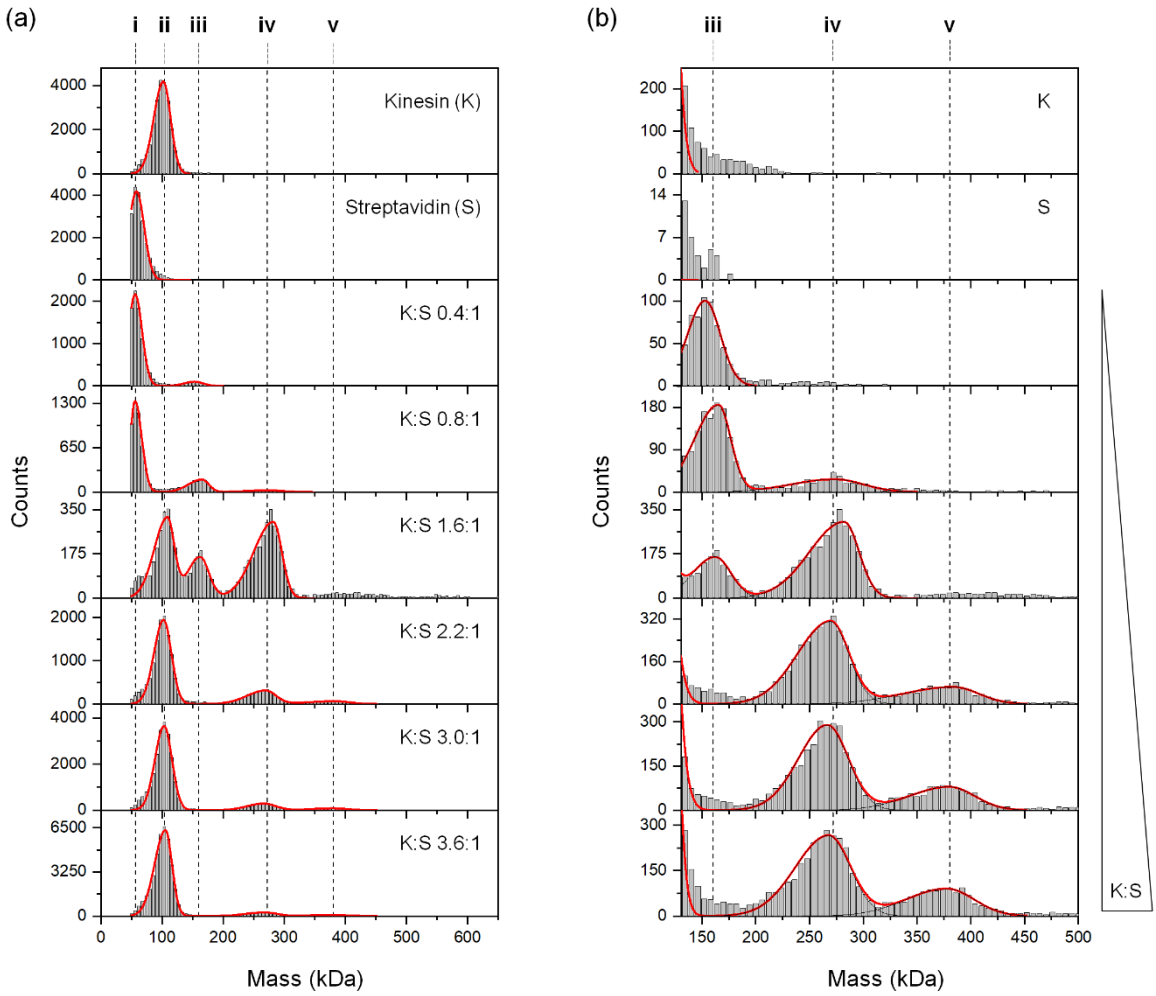

Figure 2 (a) Distributions of molecular masses revealed by mass photometry, for solutions containing kinesin (K), streptavidin (S), and their mixtures (K:S). K:S indicates the molar ratio of kinesin dimers to streptavidin tetramers in the incubation ("incubation ratio"). The concentration of streptavidin in each mixture was kept constant at 0.6 µM. Vertical dashed lines indicate molecular masses of identified major species; red solid lines indicate best fits of mass distributions to a bi-Gaussian mixture model (Materials and Methods, ESI†). (b) Expanded view of the larger species (iii-v). Red solid lines and vertical dashed lines are as described in (a). Black solid lines indicate contributions of individual species to the fit.

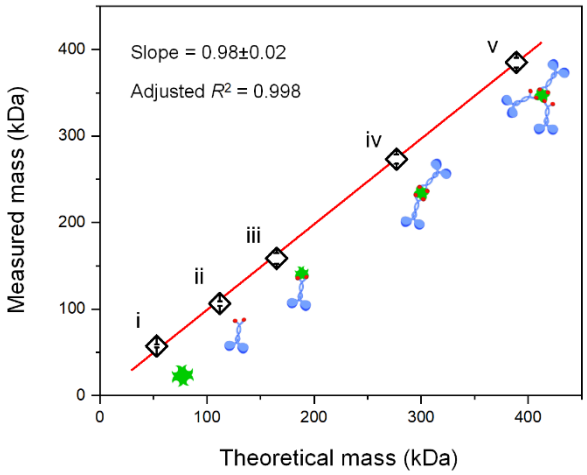

Figure 3 Theoretical vs. measured masses for major species revealed by mass photometry. Red line indicates best linear fit with zero intercept. slope = 0.98±0.02 and adjusted R2 = 0.998. Cartoons illustrate streptavidin (i), kinesin (ii), and kinesin-streptavidin complexes with 1:1, 2:1, and 3:1 stoichiometry (iii, iv, and v, respectively). Measured masses were calculated as described in Materials and Methods (ESI†). Error bars indicate standard deviation. N = 4-12.

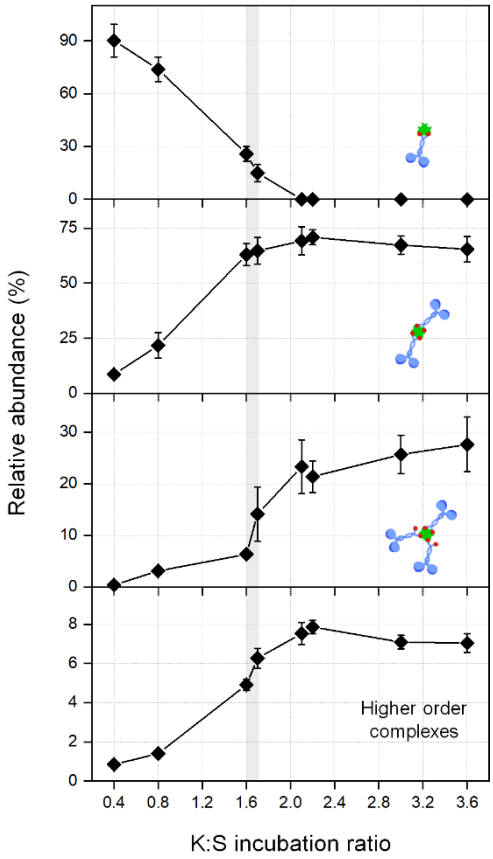

Figure 4 Relative abundances of kinesin-streptavidin complexes as a function of the kinesin: streptavidin (K: S) incubation ratio. The concentration of streptavidin in each mixture was kept constant at 0.6 µM. Cartoons illustrate kinesin-streptavidin complexes with 1:1, 2:1, and 3:1 stoichiometry (top three panels). Higher-order complexes include all measurements of mass larger than 450 kDa (Fig. S1, ESI†). Relative abundances and uncertainties were calculated as described in Materials and Methods (ESI†). Grey region highlights the incubation ratio maximizing the 2:1 complex stoichiometry.

References

1 F. J. Nedelec, T. Surrey, A. C. Maggs and S. Leibler, *Nature*, 1997, **389**, 305-308.

2 T. Sanchez, D. T. Chen, S. J. DeCamp, M. Heymann and Z. Dogic, *Nature*, 2012, **491**, 431-434.

3 G. Henkin, S. J. DeCamp, D. T. Chen, T. Sanchez and Z. Dogic, *Philos. Trans. A Math Phys. Eng. Sci.*, 2014, **372**,

4 P. Chandrakar, J. Berezney, B. Lemma, B. Hishamunda, A. Berry, K. T. Wu, R. Subramanian, J. Chung, D. Needleman, J. Gelles and Z. Dogic, *Soft Matter*, 2022, **18**, 1825-1835.

5 T. E. Bate, M. E. Varney, E. H. Taylor, J. H. Dickie, C. C. Chueh, M. M. Norton and K. T. Wu, *Nat. Commun.*, 2022, **13**, 6573.

6 A. M. Tayar, L. M. Lemma and Z. Dogic, *Methods Mol. Biol.*, 2022, **2430**, 151-183.

7 T. Surrey, F. Nedelec, S. Leibler and E. Karsenti, *Science*, 2001, **292**, 1167-1171.

8 E. Berliner, H. K. Mahtani, S. Karki, L. F. Chu, J. E. Cronan, Jr. and J. Gelles, *J. Biol. Chem.*, 1994, **269**, 8610-8615.

9 R. Subramanian and J. Gelles, *J. Gen. Physiol.*, 2007, **130**, 445-455.

10 L. Deng, E. N. Kitova and J. S. Klassen, *J. Am. Soc. Mass Spectrom.*, 2013, **24**, 49-56.

11 A. Chilkoti and P. S. Stayton, *Journal of the American Chemical Society*, 1995, **117**, 10622-10628.

12 J. Xu, B. J. Reddy, P. Anand, Z. Shu, S. Cermelli, M. K. Mattson, S. K. Tripathy, M. T. Hoss, N. S. James, S. J. King, L. Huang, L. Bardwell and S. P. Gross, *Nat Commun*, 2012, **3**, 754.

13 S. Beretta, L. Lunelli, G. Chirico and G. Baldini, *Appl. Opt.*, 1996, **35**, 3763-3770.

14 J. Stetefeld, S. A. McKenna and T. R. Patel, *Biophys Rev*, 2016, **8**, 409-427.

15 H. Zhang and P. Guo, *Methods*, 2014, **67**, 169-176.

16 P. Kukura, H. Ewers, C. Muller, A. Renn, A. Helenius and V. Sandoghdar, *Nat. Methods*, 2009, **6**, 923-927.

17 J. Ortega-Arroyo and P. Kukura, *Phys. Chem. Chem. Phys.*, 2012, **14**, 15625-15636.

18 M. Liebel, J. T. Hugall and N. F. van Hulst, *Nano Lett.*, 2017, **17**, 1277-1281.

19 D. Cole, G. Young, A. Weigel, A. Sebesta and P. Kukura, *ACS Photonics*, 2017, **4**, 211-216.

20 G. Young, N. Hundt, D. Cole, A. Fineberg, J. Andrecka, A. Tyler, A. Olerinyova, A. Ansari, E. G. Marklund, M. P. Collier, S. A. Chandler, O. Tkachenko, J. Allen, M. Crispin, N. Billington, Y. Takagi, J. R. Sellers, C. Eichmann, P. Selenko, L. Frey, R. Riek, M. R. Galpin, W. B. Struwe, J. L. P. Benesch and P. Kukura, *Science*, 2018, **360**, 423-427.

21 Refeyn Ltd, *OneMP (version 1.3) User Manual*.

22 D. Wu and G. Piszczek, *Anal. Biochem.*, 2020, **592**, 113575.

23 L. Chaiet and F. J. Wolf, *Arch. Biochem. Biophys.*, 1964, **106**, 1-5.

24 N. M. Green, *Adv. Protein Chem.*, 1975, **29**, 85-133.

25 S. R. Norris, S. Jung, P. Singh, C. E. Strothman, A. L. Erwin, M. D. Ohi, M. Zanic and R. Ohi, *Nat. Commun.*, 2018, **9**, 2659.

26 T. D. Ross, H. J. Lee, Z. Qu, R. A. Banks, R. Phillips and M. Thomson, *Nature*, 2019, **572**, 224-229.

27 B. Edozie, S. Sahu, M. Pitta, A. Englert, C. F. do Rosario and J. L. Ross, *Soft Matter*, 2019, **15**, 4797-4807.

28 L. M. Lemma, M. Varghese, T. D. Ross, M. Thomson, A. Baskaran and Z. Dogic, *PNAS Nexus*, 2023, **2**, pgad130.